

ARTICLES

Charge transfer mechanism of hydrogen-induced intergranular embrittlement of iron

Liping Zhong,^{1,2} Ruqian Wu,³ A. J. Freeman,^{1,*} and G. B. Olson⁴¹Department of Physics and Astronomy, Northwestern University, Evanston, Illinois 60208²Seagate Technology LLC, 7801 Computer Avenue South, Bloomington, Minnesota 55435³Department of Physics and Astronomy, California State University at Northridge, Northridge, California 91330⁴Department of Materials Science and Engineering, Northwestern University, Evanston, Illinois 60208

(Received 28 October 1999)

Impurity-induced reduction of intergranular cohesion—a major factor limiting the usable strength level of ultrahigh-strength steels—is particularly severe when aggravated by mobile hydrogen through environmental interaction, as in the case of hydrogen stress corrosion cracking. As an aid in establishing an understanding on the electronic level, the influence of hydrogen on the cohesion of an iron grain boundary was determined using the full-potential linearized augmented plane wave (FLAPW) method with the generalized gradient approximation. Through precise calculations on both grain boundary and free surface environments, we found that hydrogen is a strong embrittler. Analysis of the results in terms of structural relaxation, bonding character, and magnetic interactions shows that the hydrogen-iron chemical bond is stronger on the free surface and a charge-transfer mechanism is found to play a dominant role for the hydrogen-induced reduction of cohesion across the iron grain boundary. These results provide a quantitative explanation from first principles for the technologically important phenomenon of hydrogen-induced intergranular embrittlement.

H-induced embrittlement of steels remains a highly complex unsolved problem.¹ Various mechanisms have been proposed² to explain the H-induced embrittlement (HIE), such as (i) precipitation of gaseous hydrogen, (ii) formation of hydrides, (iii) deformation localization, and (iv) reduction of cohesion across the grain boundary. While the role of the first two factors has been confirmed in some systems, the relevance of the latter two is still controversial.

It has been well established that H atoms, like many other nonmetal or metalloid impurities in Fe, segregate to the Fe grain boundary (GB).^{1,2} In addition, H in Fe has a uniquely high mobility (compared to other metalloid impurities such as P and S, the mobility of H can be orders of magnitude higher). From a thermodynamic point of view, a normal segregant inevitably alters cohesion in a local environment. Based on a plausible thermodynamic description by Rice and Wang,³ the fracture mode of solids is determined by the competition between brittle interfacial cleavage separation and crack-tip blunting through dislocation emission. It has been proposed^{3,4} that for a fixed boundary solute (impurity) coverage, Γ , nonlinear entropy contributions can be neglected and thus the relation

$$2\gamma_{int} = (2\gamma_{int})_0 - (\Delta g_b^0 - \Delta g_s^0)\Gamma \quad (1)$$

holds, where $(2\gamma_{int})_0$ is the work to separate the clean grain boundary, and Δg_b^0 and Δg_s^0 are the free energies of segregation of the solute to the grain boundary and free surface (FS), respectively. Hence, if the free energy of segregation for the solute atom at the FS is more negative than it is at the GB, this positive energy difference for $\Delta g_b^0 - \Delta g_s^0$, will lead to embrittlement.

Rice and Wang³ also showed that intergranular fracture toughness is a monotonic function of the ideal work of Eq. (1) and demonstrated a compelling correlation between measured embrittlement potencies of segregants and corresponding $\Delta g_b^0 - \Delta g_s^0$ values from available surface thermodynamic data. They further predicted the manner in which the embrittlement potency of a mobile solute is amplified beyond that of Eq. (1) and used critical experiments in bicrystals (including boundaries of the geometry considered in this paper) to verify the predicted temperature dependence of intergranular hydrogen embrittlement, which can be nonmonotonic in nature through a competition between thermodynamic and kinetic factors.² Their analysis reveals that the more complex embrittlement behavior of a mobile segregant is still fundamentally driven by the thermodynamic quantity $\Delta g_b^0 - \Delta g_s^0$. Obviously, the value of $\Delta g_b^0 - \Delta g_s^0$ is intrinsically related to the interatomic chemical interaction and thus can be determined using present state-of-the-art *ab initio* quantum mechanical calculations⁵ provided the method employed treats both the GB and FS at the same level of precision.

We report here the results of precise calculations of the electronic and magnetic properties of the H/Fe $\Sigma 3[1\bar{1}0]$ (111) GB (Ref. 6) and the corresponding H/Fe(111) free surface. The mechanism of the H-induced embrittlement is investigated through a comparison of total energies, chemical bonding behavior, and magnetic interactions at 0 K. As sketched in Fig. 1(a), a 23 layer slab is adopted to simulate the clean Fe $\Sigma 3[1\bar{1}0]$ (111) GB; the H impurity is placed at the center of the trigonal prism formed by Fe host atoms. As shown in Fig. 1(b), the H/Fe(111) free surface is simulated

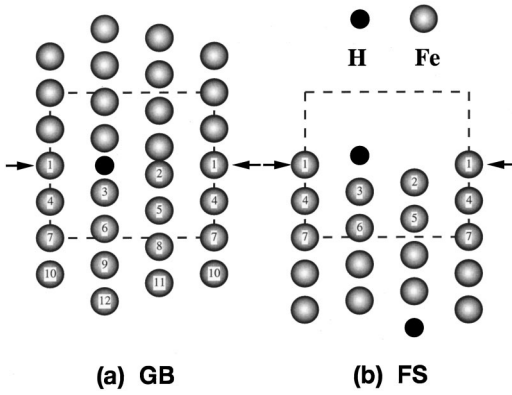


FIG. 1. Model and notation for the atomic structures of (a) Fe $\Sigma 3[1\bar{1}0]$ (111) grain boundary, and (b) Fe(111) free surface. The dashed lines mark the region mapped in Fig. 2. The arrows denote grain boundary plane and corresponding fracture surface.

by a 13 layer slab that contains a bcc Fe(111) substrate film covered by a pseudomorphic H monolayer on each side. The two-dimensional (2D) lattice constant and the unrelaxed Fe-Fe interatomic distance are chosen from experimental values for bulk bcc Fe, i.e., $d_{Fe-Fe} = 4.69$ a.u., whereas the final equilibrium atomic geometries are optimized through the calculated atomic force⁷ on each atom.

Both the GB and FS are treated by the highly precise all-electron full potential linearized augmented plane wave (FLAPW) method⁵ with the generalized gradient approximation (GGA) (Ref. 8) for the exchange and correlation interactions between electrons. No assumptions are made in the FLAPW calculations about the nature of bonding, or shape of the wave functions, charge density or potential, and are self-consistent fully converged (as also found in previous extensive tests on similar systems.^{9,11,12}

The equilibrium atomic structures were obtained by determining the vertical interplanar distances according to the calculated atomic forces for both H/Fe GB and FS as well as for the corresponding clean reference systems. The structure within the lateral (111) planes was kept unchanged in order to maintain the in-plane threefold rotational symmetry. We fixed the three outermost Fe layers while adjusting the GB and FS alters the atomic positions of the surroundings very slightly. Compared to the structure in the clean Fe GB, the Fe(2) and Fe(3) atoms are pushed away by 0.03 a.u. and 0.08 a.u. from the central plane (relative to the clean Fe GB). Compared with the metalloid impurities case,¹¹ where the impurity on the Fe(111) FS induces a strong multilayer relaxation in the substrate, the H induced relaxation is only within 0.11 a.u.

Strikingly, we found that the H-Fe bond length is much shorter in the FS environment than in the GB; the calculated $d_{H-Fe(3)}$ in H/Fe(111) is 3.12 a.u., which is about 8% shorter than that in the GB environment (3.40 a.u.), and is expected to significantly affect the chemical interactions in GB and FS. As presented in Fig. 2, the charge density differences between the self-consistent charge density of the H/Fe systems and the corresponding superpositions of the charge densities of the reference systems [i.e., a free H monolayer, the clean Fe GB and Fe(111) FS], indicate pronounced charge redistributions in both GB and FS environ-

ments. Significant charge accumulations around the H sites can be seen from the contours in Fig. 2, which show that the H in both GB and FS acts as an electron acceptor. Compared with the typical embrittling metalloid impurity P, where the P-Fe bonding undergoes a nonhybridized embeddedlike electrostatic interaction,¹¹ the contour profile in Fig. 2 suggests that the H-Fe(3) bonding is more ioniclike, which is consistent with an earlier GB calculation.¹⁰ Within the muffin-tin spheres ($r_{MT} = 1.0$ a.u.), the integral charges obtained from Fig. 2 are 0.07 and 0.11 electrons for H in the GB and FS, respectively. In the GB case, the presence of H leads to a decrease of charge density in the region between Fe(2) atoms across the GB core, as also seen for other metalloid impurities.^{12,13} With a shorter H-Fe(3) distance, the chemical interaction between H and Fe(3) atoms in the FS is much stronger than their counterpart in the GB, as also evidenced by the integral charges in the muffin-tin spheres. Strikingly, even in the vacuum in Fig. 2(b), the presence of H results in charge removal in the region above the H adatom, which indicates a much stronger H-Fe chemical interaction in FS.

This ioniclike bonding behavior can be understood from examining more fundamental electronic and magnetic properties. In fact, the basic atomic characteristics that control the impurity-host interaction are the radial extension and the relative energy position of the impurity valence states: the former is important in the covalent bond-formation ability of the impurity; the latter determines the relative amounts of ionic and covalent character in the bonding. In the case of H, the $1s$ valence orbitals are too extended to form stable covalent hybrids with the Fe host in both GB and FS. In contrast, since the energy location of H- $1s$ is much lower than the d bands of the Fe host, the bonding behavior between H and Fe is expected to be more ioniclike than covalent.

The effect of H on the magnetization of the Fe host is similar to that of C in the Fe GB and FS,¹¹ namely, a reduction on Fe(1) and Fe(3) and an enhancement on Fe(2) atoms. Referring to the clean Fe GB, the H reduces the magnetic moment of Fe(3) and Fe(1) by $0.23\mu_B$ and $0.07\mu_B$, respectively. By contrast, the H-induced magnetic moment enhancement is remarkable for Fe(2) (by $0.22\mu_B$), Fe(4) (by $0.13\mu_B$), and even for Fe(6) (by $0.05\mu_B$). At the FS, the reduction of the Fe(3) magnetic moment is as large as $0.27\mu_B$. In both environments, a small induced magnetic moment ($-0.01\mu_B$) is found in the H muffin-tin sphere.

The binding energies for a H impurity in the Fe GB and on the Fe(111) surface are calculated and their differences are given in Table I. The calculated results using the FLAPW method with the local spin density approximation (LSDA) for the exchange and correlation interactions between electrons are also listed for comparison. Results are listed for the “chemical” interaction contribution (defined as the result obtained without structural relaxation, called “unrelaxed” in Table I), the “mechanical” energy released during the structural relaxation of the clean Fe GB and FS after impurity removal (called “relaxation” in Table I), and the sum of these contributions that defines the total interaction energy. Although the impurity segregation energies used in the Rice-Wang model are expressed relative to an impurity in dilute solution in crystalline Fe, the binding energies, ΔE_b and ΔE_s , computed here are referred to the calculated binding energy of an isolated 2D monolayer with the same structure

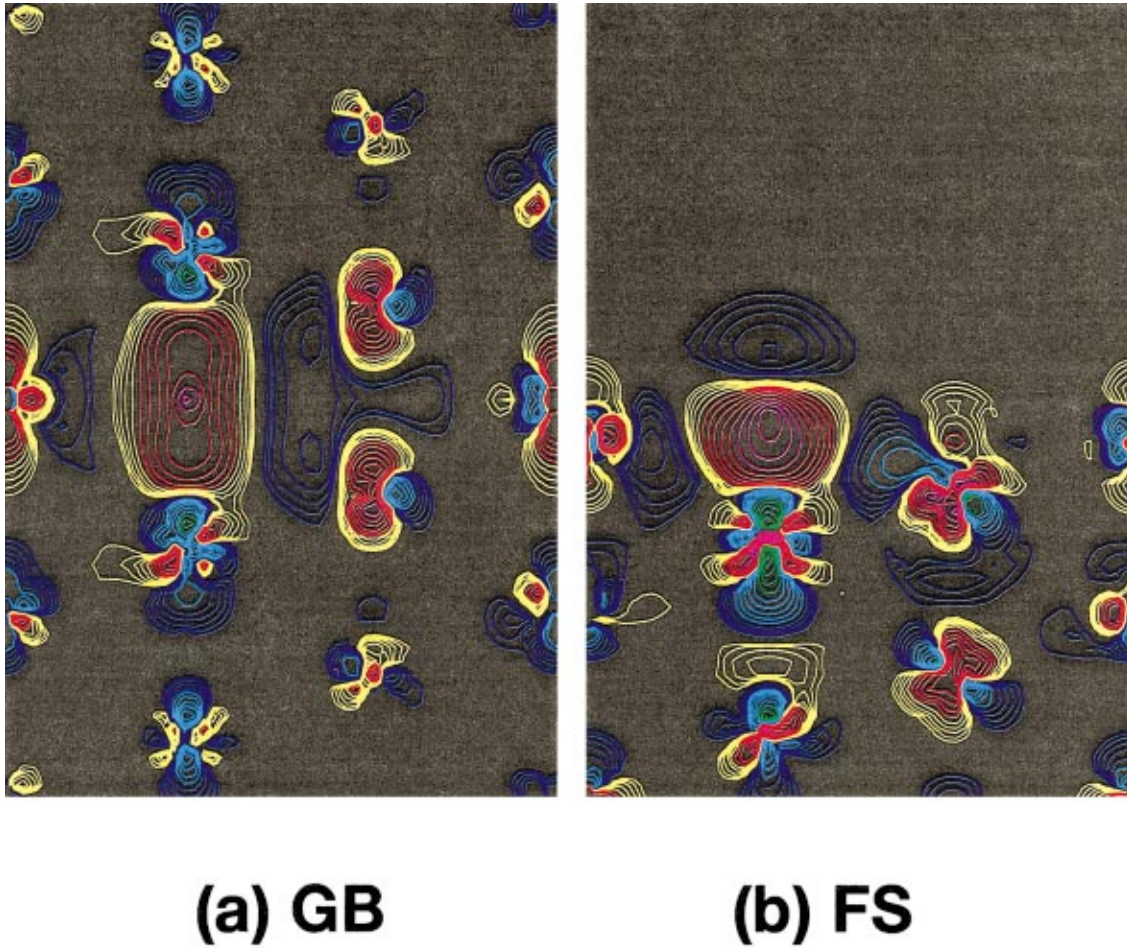


FIG. 2. (Color) The valence charge density difference calculated by FLAPW with GGA for (a) H/Fe GB and (b) H/Fe FS. Contours start from $\pm 5 \times 10^{-4}$ e/a.u.³ and increase successively by a factor of $\sqrt{2}$; yellow, red, and pink colors denote charge accumulation, and green, light blue, and dark blue denote charge depletion.

as the segregated monolayer as shown in Fig. 1. The segregation energy differences, which governing the effect of the impurity on the Fe GB cohesion, will be the same as the energy difference $\Delta E_b - \Delta E_s$. By including the H-induced structural relaxation, the binding energy ΔE_b and ΔE_s , when calculated with GGA, are -3.01 eV/adatom and -3.27 eV/adatom for H in the Fe GB and FS environments, respectively. As a result, the calculated binding-energy difference ($\Delta E_b - \Delta E_s$) is $+0.26$ eV/adatom (or 25.21 kJ/mol), which agrees well with the 25 ± 19 kJ/mol estimated from experimental data.⁴ According to the Rice-Wang thermodynamic theory,³ H is thus a strong embrittler for the cohesion across the Fe GB.

From Table I, we see that the atomic relaxation in both the clean GB and FS environments calculated with GGA has only a minimal contribution to ΔE_b and ΔE_s (0.08 and 0.15 eV/adatom respectively) and even a negative difference (-0.07 eV/adatom). By contrast, the chemical energy contributes a positive value of $\Delta E_b - \Delta E_s$ ($+0.33$ eV/adatom); it is larger in the FS than in the GB, despite the fact that one out of two vertical bonds is broken. As discussed above, this is because of the shortened H-Fe bond-length associated with the much stronger H-Fe interaction in the FS environment, which favors greater FS stability and hence an embrittling effect. This result further supports the argument that charge-

TABLE I. Binding energies (in eV) and their differences for H in Fe GB and FS and the decomposition into chemical, mechanical contributions calculated with LSDA and GGA.

		ΔE_b	ΔE_s	$\Delta E_b - \Delta E_s$
Unrelaxed (chemical)	LSDA	-3.64	-3.85	$+0.21$
	GGA	-3.09	-3.42	$+0.33$
Relaxation (mechanical)	LSDA	$+0.23$	$+0.11$	$+0.12$
	GGA	$+0.08$	$+0.15$	-0.07
Relaxed (total)	LSDA	-3.41	-3.74	$+0.33$
	GGA	-3.01	-3.27	$+0.26$

transfer from Fe to H is the key mechanism for HIE in the Fe GB.

Before discussing our results further, it is important to make comparison for the results calculated by GGA with those by LSDA. It is well known that the most widely used LSDA overestimates bulk moduli and underestimates volumes of 3d transition metal bulk solids. Of its most widely studied shortcomings is the incorrect prediction of an anti-ferromagnetic fcc ground state for Fe bulk solid, rather than the ferromagnetic bcc structure.¹³ It is well documented that the GGA is a significant improvement over LSDA on the properties governed by a realistic description of bond formation,⁸ especially in the case of Fe. Hence, we expect that in these systems, the GGA approach is more preferred. Indeed, for the GB and FS systems considered here, we can see from Table I that the calculations with GGA and with LSDA give different ΔE_b and ΔE_s values. For the energy differences, which is crucial for determining the cohesion properties of H in GB, remarkably improvement is made in the mechanical (relaxation) part. The $\Delta E_b - \Delta E_s$ calculated with LSDA is +0.12 eV, which means a contribution to embrittlement; the counterpart calculated with GGA gives -0.07 eV, which indicates even a slight enhancement for Fe GB cohesion. From the calculation with GGA, we can see more clearly that only the chemical part contributes the HIE in the Fe GB.

It is interesting to compare the HIE in the GB with the effects of other embrittling metalloid impurities such as P, where the electrostatic embeddedlike P-Fe bond is found to tune the embrittlement behavior.¹¹ For P, because of the large spatial extension of its 3p wave functions, the valence states can be easily affected by the surrounding Fe atoms; indeed the charge density in the inner region of the P atom is significantly decreased. Meanwhile the Coulomb and Pauli

repulsions push the P 3p wave function away from the high charge density region around the Fe atoms. The net action from these two effects is to squeeze the P 3p electrons into the region intermediate between P and Fe. Thus, the P-Fe bond shows the nature of an embeddedlike electrostatic interaction in which the P-Fe(1) bonding is almost as strong as the P-Fe(3) bonding. With the spatial isotropy of embeddedlike P-Fe bonds, the energy loss due to fracture is small and can be easily compensated through release of the lattice stress (mechanical relaxation) since only one out of five bonds is cut from the GB to FS.

In sharp contrast with this physical picture, the main mechanism we find for HIE is charge transfer with the H impurity acting as an electron acceptor in both the GB and FS. Although the number of neighbors of H changes from five Fe atoms [two Fe(3) and three Fe(1) atoms] in the GB to four Fe atoms [one Fe(3) and three Fe(1) atoms], in the FS the energy loss due to the removal of one Fe(3) after the fracture is compensated by enhancement of the H-Fe chemical interaction. We note that a well known early theory of hydrogen embrittlement by Troiano¹⁴ also invoked a charge-transfer mechanism, but the proposed direction of transfer was opposite to that demonstrated by the rigorous calculations presented here. In a general sense, the information obtained here may also prove to be important for investigations of H-induced effects in other alloy systems, and further electronic studies should identify new directions in alloy composition design for improved hydrogen resistance.

This work was supported by the Office of Naval Research (Grant No. N00014-94-1-0188) and a grant of computer time at the Pittsburgh Supercomputing Center from the NSF Division of Advanced Scientific Computing and the Arctic Region Supercomputing Center. We thank J. S. Wang of Harvard University for helpful discussions.

*Author to whom correspondence should be addressed. Email address: art@freeman.phys.nwu.edu

¹C. J. McMahon, Jr., in *Innovations in Ultrahigh-Strength Steel Technology*, edited by G. B. Olson, M. Azrin, and E. S. Wright, Proceedings of the 34th Sagamore Army Materials Research Conference (Government Printing Office, Washington, DC, 1990), p. 597.

²J. S. Wang, in *Hydrogen Effects in Materials*, edited by A. W. Thompson and N. R. Moody (TMS, 1966), p. 61.

³J. R. Rice and J. S. Wang, *Mater. Sci. Eng., A* **107**, 23 (1989).

⁴P. M. Anderson, J. S. Wang, and J. R. Rice, in *Innovations in Ultrahigh-Strength Steel Technology* (Ref. 1), p. 619.

⁵E. Wimmer, H. Krakauer, M. Weinert, and A. J. Freeman, *Phys. Rev. B* **24**, 864 (1981).

⁶ $\Sigma 3$ refers to a special orientation between crystals for which one in three lattice points are coincident, $[1\bar{1}0]$ denotes the crystal Miller indices of the axis of misorientation, and (111) denotes the habit plane of the boundary, both referred to the bcc crystal

lattice. The boundary corresponds to the ‘‘incoherent’’ twin boundary.

⁷J. M. Soler and A. R. Williams, *Phys. Rev. B* **40**, 1560 (1989); R. Yu, D. Singh, and H. Krakauer, *ibid.* **43**, 6411 (1992); R. Wu and A. J. Freeman (unpublished).

⁸J. P. Perdew, K. Burke, and M. Ernzerhof, *Phys. Rev. Lett.* **77**, 3865 (1996).

⁹A. J. Freeman and R. Wu, *J. Magn. Magn. Mater.* **100**, 497 (1992).

¹⁰G. L. Krasko and G. B. Olson, *Solid State Commun.* **76**, 247 (1990); **79**, 113 (1991).

¹¹R. Wu, A. J. Freeman, and G. B. Olson, *Science* **265**, 376 (1994); *Phys. Rev. B* **53**, 7504 (1996).

¹²L. Zhong, R. Wu, A. J. Freeman, and G. B. Olson, *Phys. Rev. B* **55**, 11 133 (1996).

¹³C. S. Wang, B. M. Klein, and H. Krakauer, *Phys. Rev. Lett.* **54**, 1852 (1985).

¹⁴A. R. Troiano, *Trans. Am. Soc. Met.* **52**, 54 (1960).